Thermolysis of $Ru_3(CO)_{10}[Fe(\eta\text{-}C_5H_4PPr^i_2)_2]$. Structure of $Ru_3(CO)_8(\mu\text{-}H)_2[(\eta\text{-}PC_5H_4)Fe(\eta\text{-}C_5H_4PPr^i_2)]$ and $Ru_3(CO)_8(\mu\text{-}H)(\mu\text{-}OH)[\mu\text{-}Fe(\eta\text{-}C_5H_4PPr^i_2)_2]$

William R. Cullen,* Steven J. Rettig, and Tu-cai Zheng

Department of Chemistry, University of British Columbia, Vancouver, British Columbia, Canada V6T 1Z1

Received June 4, 1991

Heating $Ru_3(CO)_{10}(Fc'(PPr^i_2)_2)$ (Fc' = $Fe(\eta\text{-}C_5H_4)_2$) in refluxing cyclohexane affords three products in moderate yields. The complex $Ru_3(CO)_8(\mu\text{-}H)_2[(\eta\text{-}PC_5H_4)Fe(\eta\text{-}C_5H_4PPr^i_2)]$ (7) was characterized by X-ray diffraction. It crystallizes in the triclinic system, space group $P\bar{1}$, with a = 11.782 (4) Å, b = 12.538 (5) Å, c = 10.193 (6) Å, α = 95.70 (4)°, β = 98.70 (4)°, γ = 84.41 (3)°, and Z = 2; the final R value of 0.027 was obtained by using 6083 observed reflections. The phosphinidene group caps one face of the Ru_3 triangle. The two bridging hydrides were located in the structure refinement. One side product, $Ru_3(CO)_8(\mu\text{-}Cl)(\mu\text{-}OH)[\mu\text{-}Fc'(PPr^i_2)_2]$ (9), was also characterized by X-ray diffraction. It crystallizes in the monoclinic system, space group $P2_1/n$, with a = 16.330 (2) Å, b = 11.651 (2) Å, c = 19.147 (3) Å, β = 93.34 (1)°, and Z = 4; the final R value of 0.030 was obtained by using 4910 observed reflections. The Cl, OH, and ferrocene moieties bridge the same two Ru atoms that are not otherwise connected by a metal–metal bond.

Introduction

Benzyne, C_6H_4, is a highly reactive molecule[1] that has been trapped on single- and multiple-metal centers as in **1** and **2**.[2-4] There are few reports, however, concerning

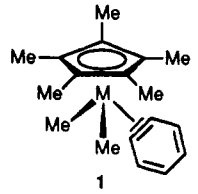

1

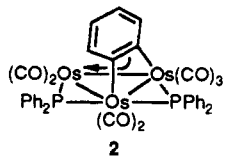

2

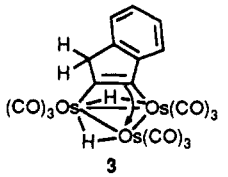

3

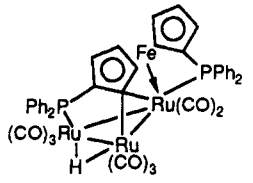

4

the possibility that ferrocyne, $Fe(\eta\text{-}C_5H_5)(\eta\text{-}C_5H_3)$, has an independent existence.[5] Work showing that complexes such as **3** are stable[6] has encouraged us to pursue the possibility of trapping ferrocyne as part of Ru_3- and Os_3-cluster complexes by using techniques similar to those used for the preparation of **2**. The products of the pyrolysis of $Ru_3(CO)_{10}(PFcPh_2)_2$[3j] (FcH = $Fe(\eta\text{-}C_5H_5)_2$) and $Ru_3(CO)_{10}(Fc'(PPh_2)_2)$[4a] ($Fc'$ = $Fe(\eta\text{-}C_5H_4)_2$) indicate that metalation and P–C bond cleavage are generally more facile for *P*-phenyl moieties than *P*-ferrocenyl; however, one interesting compound, **4**, containing a metalated C_5 ring and a novel Fe–Ru bond, was obtained and characterized crystallographically.[4a] It is generally established that the order C(sp) > C(sp^2) > C(sp^3) applies to the ease of cleavage of both P–C and C–H bonds;[7] therefore, to enhance the possibility of preparing derivatives of ferrocyne, we decided to study the pyrolytic reactions of alkylferrocenylphosphine complexes of Ru_3 and Os_3 clusters. Here we present our studies on the pyrolysis of $Ru_3(CO)_{10}(Fc'(PPr^i_2)_2)$. Unexpectedly, the compounds isolated show both P–C(sp^3) and P–C(sp^2) bond cleavage and Fe→Ru bond formation.

Experimental Section

All reactions were carried out under an argon atmosphere by using standard Schlenk techniques. Solvents were predried and freshly distilled. Both ^1H and ^{31}P NMR spectra (Table VIII) were recorded by using either a Bruker WM-400 or a Varian XL-300 spectrometer. ^{31}P chemical shifts are listed relative to 85% H_3PO_4. FAB mass spectra were acquired by using an AEI MS-9 spectrometer. Argon was used as the exciting gas and 3-nitrobenzyl alcohol as the matrix, and the sample was dissolved in acetone or dichloromethane. Microanalyses were performed by Mr. Peter Borda of this department.

Preparation of $Ru_3(CO)_{10}[Fc'(PPr^i_2)_2]$ (5). $Ru_3(CO)_{12}$ (128 mg, 0.2 mmol) and $Fc'(PPr^i_2)_2$[8] (84 mg, 0.2 mmol) were dissolved in THF (20 mL) in a Schlenk tube. The catalyst PPN^+Cl^- ($PPN^+ = (PPh_3)_2N^+$; 10 mg) was added to the stirred solution, and the solution changed instantly from orange to dark red. The reaction was monitored by TLC and was complete in 30 min. The solvent was removed under reduced pressure, and the residue was applied to a silica chromatography column, with 3/1 petroleum ether/CH_2Cl_2 as eluent. The major dark red band was collected, and pure $Ru_3(CO)_{10}(Fc'(PPr^i_2)_2)$ was obtained in 75% yield after solvent evaporation. ^1H NMR (300 MHz, $CDCl_3$): δ 1.10–1.45

(1) (a) Huisgen, R. In *Organometallic Chemistry*; Zeiss, H., Ed.; Reinhold: New York, 1960; Chapter 2. (b) Fieser, L. F. *Organic Chemistry*; Reinhold: New York, 1961. (c) Gilchrist, T. L.; Rees, C. W. *Carbenes, Nitrenes, and Arynes*; Nelson and Sons: London, 1969.

(2) E.g.: (a) Bennett, M. A.; Hambley, T. W.; Roberts, N. K.; Robertson, G. B. *Organometallics* **1985**, *4*, 1992. (b) McLain, S. T.; Schrock, R. R.; Sharp, P. R.; Churchill, M. R.; Youngs, W. J. *J. Am. Chem. Soc.* **1979**, *101*, 263. (c) Churchill, M. R.; Youngs, W. J. *Inorg. Chem.* **1979**, *18*, 1697. (d) Buchwald, S. L.; Watson, B. T. *J. Am. Chem. Soc.* **1986**, *108*, 7411.

(3) E.g.: (a) Gainsford, G. J.; Guss, J. M.; Ireland, P. R.; Mason, R.; Bradford, C. W.; Nyholm, R. S. *J. Organomet. Chem.* **1972**, *40*, C70. (b) Bradford, C. W.; Nyholm, R. S. *J. Chem. Soc., Dalton Trans.* **1973**, 529. (c) Bruce, M. I.; Shaw, G.; Stone, F. G. A. *J. Chem. Soc., Dalton Trans.* **1972**, 2094. (d) Demming, A. J.; Kimber, R. E.; Underhill, M. *J. Chem. Soc., Dalton Trans.* **1973**, 2589. (e) Deeming, A. J.; Rothwell, I. P.; Hursthouse, M. B.; Backer-Dirks, J. D. J. *J. Chem. Soc., Dalton Trans.* **1981**, 1879. (f) Brown, S. C.; Evans, J.; Smart, L. E. *J. Chem. Soc., Chem. Commun.* **1980**, 1021. (g) Goudsmit, R. J.; Johnson, B. F. G.; Lewis, J.; Raithby, P. R.; Rosales, M. J. *J. Chem. Soc., Dalton Trans.* **1983**, 2257. (h) Bruce, M. I.; Guss, I. M.; Mason, R.; Shelton, B. W.; White, A. H. *J. Organomet. Chem.* **1983**, *251*, 261. (i) Deeming, A. J.; Kabir, S. E.; Powell, N. I.; Bates, P. A.; Hursthouse, M. B. *J. Chem. Soc., Dalton Trans.* **1987**, 1520. (j) Cullen, W. R.; Chacon, S. T.; Bruce, M. I.; Einstein, F. W. B.; Jones, R. H. *Organometallics* **1988**, *7*, 2273.

(4) (a) Bruce, M. I.; Cullen, W. R.; Humphrey, P. A.; Shawkataly, O. B.; Snow, M. R.; Tiekink, E. R. T. *Organometallics* **1990**, *9*, 2910. (b) Knox, S. A. R.; Lloyd, B. R.; Orpen, A. G.; Vinas, J. M.; Weber, M. *J. Chem. Soc., Chem. Commun.* **1987**, 1498.

(5) (a) Huffman, J. W.; Cope, J. F. *J. Org. Chem.* **1971**, *36*, 4068. (b) Huffman, J. W.; Keith, L. H.; Asbury, R. L. *J. Org. Chem.* **1965**, *30*, 1600.

(6) (a) Deeming, A. J. *J. Organomet. Chem.* **1978**, *150*, 123. (b) Yin, C. C.; Deeming, A. J. *J. Chem. Soc., Dalton Trans.* **1982**, 2563. (c) Humphries, A. P.; Knox, S. A. R. *J. Chem. Soc., Dalton Trans.* **1975**, 1710.

(7) Garrou, P. E. *Chem. Rev.* **1985**, *85*, 171.

(8) The synthesis follows the same procedure used for $Fc'(PPh_2)_2$[4a] except $ClPPr^i_2$ is substituted for $ClPPh_2$.

0276-7333/92/2311-0853$03.00/0

Table I. Crystallographic Data[a] for 7 and 9

compd	7	9
formula	$C_{24}H_{24}FeO_8P_2Ru_3$	$C_{30}H_{37}ClFeO_9P_2Ru_3$
fw	861.45	1001.64
color, habit	red-orange, prism	orange, prism
cryst size, mm	0.20 × 0.35 × 0.45	0.10 × 0.28 × 0.45
cryst syst	triclinic	monoclinic
space group	$P\bar{1}$	$P2_1/n$
a, Å	11.782 (4)	16.330 (2)
b, Å	12.538 (5)	11.651 (2)
c, Å	10.193 (6)	19.147 (3)
α, deg	95.70 (4)	90
β, deg	98.70 (4)	93.34 (1)
γ, deg	84.41 (3)	90
V, Å^3	1476 (1)	3637 (1)
Z	2	4
ρ_{calc}, g/cm^3	1.938	1.829
$F(000)$	840	1984
μ(Mo Kα), cm^{-1}	21.09	17.28
transmissn factors	0.74–1.00	0.79–1.00
scan type	ω–2θ	ω–2θ
scan range in ω, deg	1.26 + 0.35 tan θ	1.00 + 0.35 tan θ
scan rate, deg/min	16	16
data collected	$+h,\pm k,\pm l$	$+h,+k,\pm l$
$2\theta_{max}$, deg	60	55
cryst decay, %	negligible	2.1
total no. of rflns	9004	9050
no. of unique rflns	8614	8743
R_{merge}	0.042	0.027
no. of rflns with $I \geq 3\sigma(I)$	6083	4910
no. of variables	347	419
R	0.027	0.030
R_w	0.034	0.034
GOF	1.29	1.18
max Δ/σ (final cycle)	0.05	0.01
residual density, e/Å^3	−0.47 to +0.90 (near Ru)	−0.44 to +0.53

[a] Conditions and additional details: temperature 294 K, Rigaku AFC6S diffractometer, Mo Kα radiation (λ = 0.71069 Å), graphite monochromator, takeoff angle 6.0°, aperture 6.0 × 6.0 mm at a distance of 285 mm from the crystal, stationary background counts at each end of the scan (scan/background time ratio 2:1, up to 8 rescans), $\sigma^2(F^2) = [S^2(C + 4B) + (PF^2)^2]/Lp^2$ (S = scan rate, C = scan count, B = normalized background count, P = 0.035 for 7, 0.03 for 9), function minimized $\sum w(|F_o| - |F_c|)^2$, where $w = 4F_o^2/\sigma^2(F_o^2)$, $R = \sum||F_o| - |F_c||/\sum|F_o|$, $R_w = (\sum w(|F_o| - |F_c|)^2/\sum w|F_o|^2)^{1/2}$, and GOF = $[\sum w(|F_o| - |F_c|)^2/(m - n)]^{1/2}$. Values given for R, R_w, and GOF are based on those reflections with $I \geq 3\sigma(I)$.

(m, 24 H), 2.30–2.55 (m, 4 H), 4.35–4.45 (m, 4 H), 4.45–4.55 (m, 4 H). $^{31}P\{^1H\}$ NMR (121.4 MHz, $CDCl_3$): δ 41.3. FAB mass spectrum: m/e 1001 (P^+), 973, 945, 917, 889 (base peak), 861, 833, 818, 805, 790, 777, 762, 749, 734, 721, 706, 693, 678, 661, 650, 629, 589, 562, 549. Anal. Calcd for $C_{32}H_{36}FeO_{10}P_2Ru_3$: C, 38.37; H, 3.62. Found: C, 38.40; H, 3.77.

Pyrolysis of $Ru_3(CO)_{10}[Fc'(PPr^i_2)_2]$ (5). The complex (200 mg, 0.2 mmol) was dissolved in cyclohexane (100 mL), and the solution was refluxed for 15 h with stirring. (The reaction was monitored by TLC, and decomposition was detected after 2 h.) The solvent was removed under reduced pressure, and the residue was subjected to column chromatography (silica, 3/1 petroleum ether/CH_2Cl_2 as eluent). Two major bands were eluted by using this solvent system, and a minor one was eluted by using CH_2Cl_2. The first major band was subsequently resolved into two bands containing 6 and 7 (silica, 3/1 petroleum ether/diethyl ether as eluent). The second major band contained 8, while the minor band contained 9. The approximate yields were as follows: 6, 15%; 7, 25%; 8, 20%; 9, 1%. Spectroscopic data are listed in Table VIII. Analytical data are as follows: Calcd for $C_{27}H_{30}FeO_8P_2Ru_3$ (6): C, 35.89; H, 3.35. Found: C, 36.04; H, 3.45. Calcd for $C_{24}H_{24}FeO_8P_2Ru_3$ (7): C, 33.46; H, 2.81. Found: C, 33.20; H, 2.75. Calcd for $C_{30}H_{37}ClFeO_9P_2Ru_3$ (9): C, 36.10; H, 3.74; Cl, 3.55. Found: C, 35.89; H, 3.62; Cl, 3.20.

X-ray Crystallographic Analyses. Crystallographic data for $[\mu_3\text{-}\eta^3\text{:}\eta^1\text{-}(\eta\text{-}C_5H_4P)(\eta\text{-}C_5H_4PPr^i_2)Fe](\mu\text{-}H)_2Ru_3(CO)_8(3Ru\text{–}Ru)$ (7) and $[\mu\text{-}\eta^1\text{:}\eta^1\text{-}(\eta\text{-}C_5H_4PPr^i_2)_2Fe](\mu\text{-}Cl)(\mu\text{-}OH)Ru_3(CO)_8(2Ru\text{–}Ru)$ (9) appear in Table I. The final unit-cell parameters were obtained by least squares on the setting angles for 25 reflections with 2θ = 29.8–33.7° for 7 and 20.5–28.3° for 9. The intensities of three standard reflections, measured every 200 reflections throughout the data collections, remained constant for 7 and decayed uniformly by 2.1% for 9. The data were processed[9] and corrected for Lorentz and polarization effects, decay (for 9), and absorption (empirical, based on azimuthal scans for four reflections).

Table II. Atomic Coordinates (Fractional) and B_{eq} Values (Å^2) for 7 (Esd's in Parentheses)

atom	x	y	z	B_{eq}
Ru(1)	0.28391 (2)	0.29751 (2)	0.38203 (2)	2.769 (8)
Ru(2)	0.47173 (2)	0.37077 (2)	0.26120 (2)	3.09 (1)
Ru(3)	0.25217 (2)	0.36885 (2)	0.10718 (2)	3.31 (1)
Fe	0.29198 (4)	−0.02488 (3)	0.18486 (5)	3.40 (2)
P(1)	0.36338 (6)	0.22690 (5)	0.19558 (7)	2.81 (3)
P(2)	0.13650 (7)	0.18070 (7)	0.36893 (8)	3.34 (3)
O(1)	0.4518 (3)	0.1568 (2)	0.5544 (3)	6.2 (1)
O(2)	0.2060 (3)	0.4696 (3)	0.5927 (4)	8.2 (2)
O(3)	0.6839 (3)	0.2936 (4)	0.4461 (4)	8.3 (2)
O(4)	0.4572 (3)	0.6173 (2)	0.3122 (3)	5.9 (1)
O(5)	0.6070 (3)	0.3605 (3)	0.0297 (3)	7.3 (2)
O(6)	0.0411 (3)	0.2794 (5)	−0.0556 (4)	10.5 (3)
O(7)	0.1953 (4)	0.6132 (3)	0.1420 (5)	9.8 (2)
O(8)	0.3534 (3)	0.3594 (3)	−0.1489 (3)	7.9 (2)
C(1)	0.3873 (3)	0.0888 (2)	0.1380 (3)	3.2 (1)
C(2)	0.4592 (3)	0.0090 (3)	0.2087 (4)	3.9 (1)
C(3)	0.4457 (3)	−0.0914 (3)	0.1342 (4)	4.9 (2)
C(4)	0.3680 (4)	−0.0741 (3)	0.0184 (4)	4.9 (2)
C(5)	0.3307 (3)	0.0361 (3)	0.0200 (3)	4.3 (1)
C(6)	0.1733 (3)	0.0425 (2)	0.3036 (3)	3.6 (1)
C(7)	0.2516 (3)	−0.0351 (3)	0.3703 (4)	4.7 (2)
C(8)	0.2450 (4)	−0.1358 (3)	0.2951 (5)	6.0 (2)
C(9)	0.1636 (4)	−0.1220 (3)	0.1807 (5)	6.0 (2)
C(10)	0.1192 (3)	−0.0137 (3)	0.1842 (4)	4.9 (2)
C(11)	0.0010 (3)	0.2138 (3)	0.2553 (4)	4.7 (2)
C(12)	−0.0450 (4)	0.3336 (4)	0.2632 (5)	6.4 (2)
C(13)	−0.0967 (3)	0.1426 (4)	0.2659 (5)	6.6 (2)
C(14)	0.0875 (4)	0.1607 (4)	0.5294 (4)	5.4 (2)
C(15)	0.1843 (5)	0.1316 (4)	0.6394 (4)	7.0 (3)
C(16)	0.0104 (5)	0.2582 (5)	0.5800 (5)	7.9 (3)
C(17)	0.3847 (3)	0.2095 (3)	0.4939 (3)	3.8 (1)
C(18)	0.2308 (3)	0.4046 (3)	0.5152 (4)	4.4 (1)
C(19)	0.6047 (3)	0.3225 (3)	0.3796 (4)	4.9 (2)
C(20)	0.4638 (3)	0.5276 (3)	0.2950 (3)	4.0 (1)
C(21)	0.5549 (3)	0.3643 (3)	0.1146 (4)	4.5 (2)
C(22)	0.1170 (4)	0.3140 (4)	0.0112 (4)	5.8 (2)
C(23)	0.2156 (4)	0.5237 (3)	0.1270 (5)	5.5 (2)
C(24)	0.3170 (3)	0.3646 (3)	−0.0522 (4)	4.8 (2)
H(1)	0.3802	0.3903	0.3796	5.1
H(2)	0.197 (3)	0.379 (3)	0.255 (4)	5 (1)

Both structures were solved by heavy-atom methods, the coordinates of the Ru and Fe atoms being determined from the Patterson functions and those of the remaining non-hydrogen atoms from subsequent difference Fourier syntheses. The structure analysis of 7 was initiated in the centrosymmetric space group $P\bar{1}$, this choice being confirmed by the subsequent successful solution and refinement of the structure. All non-hydrogen atoms of both complexes were refined with anisotropic thermal parameters. One of the metal hydride atoms in 7 and the OH hydrogen atom in 9 were refined with isotropic thermal parameters. The second metal hydride atom in 7 was included in a difference map position but could not be refined. All other hydrogen atoms in both structures were fixed in idealized positions (C–H = 0.98 Å, $B_H = 1.2B_{bonded\ atom}$). A correlation for secondary extinction was applied for 9, the final value of the extinction coefficient being 1.12×10^{-7}. Neutral atom scattering factors and anomalous dispersion corrections for the non-hydrogen atoms were taken from ref 10. Final atom coordinates and equivalent isotropic thermal parameters, bond lengths, and bond angles appear in Tables II–VII.

(9) TEXSAN/TEXRAY structure analysis package that includes versions of the following: DIRDIF, direct methods for difference structures, by P. T. Beurskens; ORFLS, full-matrix least squares, and ORFFE, function and errors, by W. R. Busing, K. O. Martin, and H. A. Levy; ORTEP II, illustrations, by C. K. Johnson.

(10) *International Tables for X-ray Crystallography*; Kynoch Press: Birmingham, U.K. (present distributor Kluwer Academic Publishers: Dordrecht, The Netherlands), 1974; Vol. IV, pp 99–102, 149.

Table III. Intramolecular Distances for 7 (Å) (Esd's in Parentheses)

Ru(1)–H(1)	1.71	Fe–C(9)	2.025 (4)
Ru(1)–H(2)	1.85 (4)	Fe–C(10)	2.027 (4)
Ru(2)–H(1)	1.72	O(1)–C(17)	1.129 (4)
Ru(3)–H(2)	1.72 (4)	O(2)–C(18)	1.127 (4)
Ru(1)–Ru(2)	2.950 (1)	O(3)–C(19)	1.120 (4)
Ru(1)–Ru(3)	2.984 (2)	O(4)–C(20)	1.118 (4)
Ru(2)–Ru(3)	2.817 (1)	O(5)–C(21)	1.129 (4)
Ru(1)–P(1)	2.305 (1)	O(6)–C(22)	1.133 (5)
Ru(2)–P(1)	2.298 (1)	O(7)–C(23)	1.124 (5)
Ru(3)–P(1)	2.281 (1)	O(8)–C(24)	1.127 (5)
Ru(1)–P(2)	2.359 (1)	P(1)–C(1)	1.782 (3)
Ru(1)–C(17)	1.874 (4)	P(2)–C(6)	1.829 (3)
Ru(1)–C(18)	1.941 (3)	P(2)–C(11)	1.862 (4)
Ru(2)–C(21)	1.898 (4)	P(2)–C(14)	1.863 (4)
Ru(2)–C(19)	1.914 (4)	C(1)–C(5)	1.418 (4)
Ru(2)–C(20)	1.958 (3)	C(1)–C(2)	1.426 (4)
Ru(3)–C(22)	1.891 (4)	C(2)–C(3)	1.414 (5)
Ru(3)–C(24)	1.891 (4)	C(3)–C(4)	1.402 (6)
Ru(3)–C(23)	1.945 (4)	C(4)–C(5)	1.407 (5)
Fe–Cp(1)	1.646 (2)	C(6)–C(10)	1.423 (5)
Fe–Cp(2)	1.623 (2)	C(6)–C(7)	1.438 (5)
Fe–C(1)	2.032 (3)	C(7)–C(8)	1.414 (6)
Fe–C(2)	2.029 (4)	C(8)–C(9)	1.407 (7)
Fe–C(3)	2.036 (4)	C(9)–C(10)	1.405 (6)
Fe–C(4)	2.051 (4)	C(11)–C(12)	1.545 (6)
Fe–C(5)	2.042 (4)	C(11)–C(13)	1.546 (6)
Fe–C(6)	2.053 (3)	C(14)–C(15)	1.518 (7)
Fe–C(7)	2.036 (4)	C(14)–C(16)	1.545 (7)
Fe–C(8)	2.037 (4)		

Table IV. Intramolecular Bond Angles for 7 (deg) (Esd's in Parentheses)

H(1)–Ru(1)–H(2)	82.05	C(24)–Ru(3)–P(1)	97.6 (1)
H(1)–Ru(1)–C(17)	94.98	C(24)–Ru(3)–Ru(2)	91.3 (1)
H(1)–Ru(1)–C(18)	81.19	C(23)–Ru(3)–P(1)	145.0 (1)
H(1)–Ru(1)–P(1)	80.71	C(23)–Ru(3)–Ru(2)	95.7 (1)
H(1)–Ru(1)–P(2)	173.64	P(1)–Ru(3)–Ru(2)	52.31 (3)
H(2)–Ru(1)–C(17)	173 (1)	C(1)–P(1)–Ru(3)	133.2 (1)
H(2)–Ru(1)–C(18)	87 (1)	C(1)–P(1)–Ru(2)	137.5 (1)
H(2)–Ru(1)–P(1)	80 (1)	C(1)–P(1)–Ru(1)	127.8 (1)
H(2)–Ru(1)–P(2)	92 (1)	Ru(3)–P(1)–Ru(2)	75.91 (4)
C(17)–Ru(1)–C(18)	99.4 (2)	Ru(3)–P(1)–Ru(1)	81.17 (5)
C(17)–Ru(1)–P(1)	92.8 (1)	Ru(2)–P(1)–Ru(1)	79.71 (4)
C(17)–Ru(1)–P(2)	91.4 (1)	C(6)–P(2)–C(11)	100.3 (2)
C(18)–Ru(1)–P(1)	159.0 (1)	C(6)–P(2)–C(14)	102.2 (2)
C(18)–Ru(1)–P(2)	98.0 (1)	C(6)–P(2)–Ru(1)	115.0 (1)
P(1)–Ru(1)–P(2)	98.76 (4)	C(11)–P(2)–C(14)	104.4 (2)
H(1)–Ru(2)–C(21)	170.71	C(11)–P(2)–Ru(1)	116.8 (1)
H(1)–Ru(2)–C(19)	95.69	C(14)–P(2)–Ru(1)	116.1 (1)
H(1)–Ru(2)–C(20)	79.42	Cp(1)–Fe–Cp(2)	175.35 (8)
H(1)–Ru(2)–P(1)	80.64	Ru(1)–H(1)–Ru(2)	118.8
H(1)–Ru(2)–Ru(3)	77.04	Ru(1)–H(2)–Ru(3)	113 (2)
C(21)–Ru(2)–C(19)	93.1 (2)	O(1)–C(17)–Ru(1)	174.4 (3)
C(21)–Ru(2)–C(20)	95.5 (2)	O(2)–C(18)–Ru(1)	175.9 (4)
C(21)–Ru(2)–P(1)	99.6 (1)	O(3)–C(19)–Ru(2)	178.2 (4)
C(21)–Ru(2)–Ru(3)	95.8 (1)	O(4)–C(20)–Ru(2)	178.4 (4)
C(19)–Ru(2)–C(20)	103.8 (2)	O(5)–C(21)–Ru(2)	178.2 (4)
C(19)–Ru(2)–P(1)	107.9 (1)	O(6)–C(22)–Ru(3)	174.0 (4)
C(19)–Ru(2)–Ru(3)	158.9 (1)	O(7)–C(23)–Ru(3)	178.1 (5)
C(20)–Ru(2)–P(1)	143.9 (1)	O(8)–C(24)–Ru(3)	177.7 (4)
C(20)–Ru(2)–Ru(3)	94.4 (1)	C(12)–C(11)–C(13)	109.9 (3)
P(1)–Ru(2)–Ru(3)	51.77 (3)	C(12)–C(11)–P(2)	115.4 (3)
H(2)–Ru(3)–C(22)	92 (1)	C(13)–C(11)–P(2)	113.6 (3)
H(2)–Ru(3)–C(24)	177 (1)	C(15)–C(14)–C(16)	109.7 (4)
H(2)–Ru(3)–C(23)	81 (1)	C(15)–C(14)–P(2)	114.2 (3)
H(2)–Ru(3)–P(1)	83 (1)	C(16)–C(14)–P(2)	112.4 (4)
H(2)–Ru(3)–Ru(2)	87 (1)	C(5)–C(1)–C(2)	107.4 (3)
C(22)–Ru(3)–C(24)	90.5 (2)	C(5)–C(1)–P(1)	126.5 (2)
C(22)–Ru(3)–C(23)	104.7 (2)	C(2)–C(1)–P(1)	125.9 (2)
C(22)–Ru(3)–P(1)	106.9 (2)	C(7)–C(6)–C(10)	106.1 (3)
C(22)–Ru(3)–Ru(2)	159.2 (2)	C(7)–C(6)–P(2)	126.2 (3)
C(24)–Ru(3)–C(23)	96.7 (2)	C(10)–C(6)–P(2)	127.3 (3)

Results and Discussion

The thermal decomposition of $Ru_3(CO)_{10}[Fc'(PPh_2)_2]$ affords products resulting predominantly from P–Ph activation and cleavage; however, others result from P–C_5-ring cleavage and one product, **4**, is essentially the result of metalation of one C_5 ring accompanied by the formation of a Fe→Ru bond. Consequently, it was of interest to study the thermolysis of related derivatives that did not contain phenyl groups. We chose to work with $Ru_3(CO)_{10}[Fe(\eta\text{-}C_5H_4PPr^i_2)_2]$ (**5**), which is easily prepared from $Ru_3(CO)_{12}$ and the ligand with the aid of the catalyst PPN^+Cl^-.

Table V. Atomic Coordinates (Fractional) and B_{eq} Values (Å²) for 9 (Esd's in Parentheses)

atom	x	y	z	B_{eq}[a]
Ru(1)	0.38360 (2)	0.53087 (3)	0.33478 (2)	2.47 (2)
Ru(2)	0.34281 (2)	0.60804 (3)	0.17933 (2)	2.28 (1)
Ru(3)	0.42348 (3)	0.75144 (3)	0.28201 (2)	3.13 (2)
Fe(1)	0.20555 (4)	0.25018 (6)	0.21474 (4)	2.69 (3)
Cl(1)	0.43501 (8)	0.4491 (1)	0.22532 (7)	3.26 (5)
P(1)	0.32827 (7)	0.3483 (1)	0.37051 (6)	2.56 (5)
P(2)	0.26067 (7)	0.4835 (1)	0.10113 (6)	2.29 (5)
O(1)	0.3348 (3)	0.6677 (4)	0.4566 (2)	6.0 (2)
O(2)	0.5472 (3)	0.5075 (5)	0.4122 (3)	8.1 (3)
O(3)	0.2506 (3)	0.8229 (3)	0.1428 (2)	4.9 (2)
O(4)	0.4599 (3)	0.6885 (4)	0.0755 (2)	6.7 (3)
O(5)	0.4478 (3)	0.9632 (4)	0.1912 (3)	6.7 (3)
O(6)	0.5006 (4)	0.8446 (6)	0.4188 (3)	12.0 (4)
O(7)	0.5809 (3)	0.6416 (4)	0.2339 (3)	7.9 (3)
O(8)	0.2476 (3)	0.8114 (4)	0.3191 (2)	5.9 (2)
O(9)	0.2784 (2)	0.5519 (3)	0.2662 (2)	2.9 (2)
C(1)	0.2837 (3)	0.2496 (4)	0.3047 (2)	2.7 (2)
C(2)	0.3249 (3)	0.2087 (4)	0.2455 (3)	3.2 (2)
C(3)	0.2828 (4)	0.1114 (5)	0.2180 (3)	4.2 (3)
C(4)	0.2149 (4)	0.0910 (4)	0.2588 (3)	4.4 (3)
C(5)	0.2146 (3)	0.1751 (5)	0.3118 (3)	3.7 (2)
C(6)	0.1950 (3)	0.3774 (4)	0.1396 (2)	2.5 (2)
C(7)	0.1412 (3)	0.3996 (4)	0.1948 (2)	2.8 (2)
C(8)	0.0866 (3)	0.3053 (5)	0.1989 (3)	3.7 (2)
C(9)	0.1054 (3)	0.2252 (5)	0.1472 (3)	3.8 (3)
C(10)	0.1718 (3)	0.2679 (4)	0.1106 (3)	3.3 (2)
C(11)	0.3515 (3)	0.6147 (5)	0.4090 (3)	3.7 (2)
C(12)	0.4845 (4)	0.5160 (5)	0.3827 (3)	4.5 (3)
C(13)	0.2842 (3)	0.7387 (4)	0.1579 (3)	3.1 (2)
C(14)	0.4140 (3)	0.6561 (4)	0.1144 (3)	3.5 (2)
C(15)	0.4379 (3)	0.8843 (5)	0.2236 (3)	4.1 (3)
C(16)	0.4725 (5)	0.8083 (6)	0.3679 (4)	6.3 (4)
C(17)	0.5211 (4)	0.6794 (5)	0.2530 (4)	4.9 (3)
C(18)	0.3122 (4)	0.7890 (5)	0.3059 (3)	3.9 (3)
C(19)	0.2448 (3)	0.3619 (4)	0.4317 (3)	3.3 (2)
C(20)	0.4045 (3)	0.2520 (5)	0.4163 (3)	3.6 (2)
C(21)	0.3152 (3)	0.4008 (4)	0.0354 (2)	2.8 (2)
C(22)	0.1814 (3)	0.5655 (4)	0.0468 (3)	3.2 (2)
C(23)	0.2766 (4)	0.4000 (5)	0.5053 (3)	4.6 (3)
C(24)	0.1773 (3)	0.4410 (5)	0.4015 (3)	4.3 (3)
C(25)	0.4762 (4)	0.2249 (5)	0.3730 (3)	5.0 (3)
C(26)	0.3671 (4)	0.1397 (5)	0.4432 (3)	5.1 (3)
C(27)	0.3530 (4)	0.4794 (5)	−0.0185 (3)	4.6 (3)
C(28)	0.3795 (3)	0.3208 (5)	0.0693 (3)	4.6 (3)
C(29)	0.1168 (3)	0.6150 (5)	0.0932 (3)	4.0 (3)
C(30)	0.1393 (4)	0.4966 (5)	−0.0135 (3)	5.0 (3)

[a] $B_{eq} = {}^8/_3\pi^2\sum\sum U_{ij}a_ia_j(\mathbf{a}_i\cdot\mathbf{a}_j)$.

The results are outlined in Scheme I, where numbered compounds have been isolated and characterized; those described by letters (e.g., A) have not. The reactions take place smoothly in refluxing cyclohexane (15 h). Thermolysis at higher temperatures results in low yields of **6–9** and other unidentified products. These reactions always afford material that remains on the chromatography column upon workup.

Structure of Compound 7. The structure of compound **7** (Figure 1) consists of a Ru_3 triangle that is bridged by two hydrides that were located in the structure refinement. The triangle is capped on one face by the phosphinidene group P(1). This phosphorus atom has lost both isopropyl groups. The other end of the ligand is intact and is bonded to Ru(1) through P(2). Formally,

Table VI. Intramolecular Distances (Å) for 9 (Esd's in Parentheses)

Ru(1)–Ru(3)	2.8506 (7)	P(1)–C(20)	1.858 (5)
Ru(2)–Ru(3)	2.8444 (6)	P(2)–C(6)	1.820 (5)
Ru(1)–P(1)	2.425 (1)	P(2)–C(21)	1.854 (5)
Ru(2)–P(2)	2.431 (1)	P(2)–C(22)	1.875 (5)
Ru(1)–Cl(1)	2.492 (1)	O(1)–C(11)	1.146 (6)
Ru(2)–Cl(1)	2.513 (1)	O(2)–C(12)	1.145 (6)
Ru(1)–O(9)	2.114 (3)	O(3)–C(13)	1.152 (6)
Ru(2)–O(9)	2.122 (3)	O(4)–C(14)	1.151 (6)
Ru(1)–C(11)	1.827 (6)	O(5)–C(15)	1.126 (6)
Ru(1)–C(12)	1.847 (6)	O(6)–C(16)	1.133 (7)
Ru(2)–C(13)	1.833 (5)	O(7)–C(17)	1.149 (7)
Ru(2)–C(14)	1.838 (5)	O(8)–C(18)	1.130 (6)
Ru(3)–C(15)	1.932 (6)	C(1)–C(2)	1.433 (7)
Ru(3)–C(16)	1.906 (7)	C(1)–C(5)	1.437 (6)
Ru(3)–C(17)	1.913 (7)	C(2)–C(3)	1.411 (7)
Ru(3)–C(18)	1.950 (6)	C(3)–C(4)	1.413 (8)
Fe(1)–Cp(1)	1.664 (3)	C(4)–C(5)	1.412 (8)
Fe(1)–Cp(2)	1.659 (2)	C(6)–C(7)	1.437 (6)
Fe(1)–C(1)	2.083 (5)	C(6)–C(10)	1.434 (6)
Fe(1)–C(2)	2.060 (5)	C(7)–C(8)	1.420 (7)
Fe(1)–C(3)	2.050 (5)	C(8)–C(9)	1.406 (8)
Fe(1)–C(4)	2.039 (5)	C(9)–C(10)	1.415 (7)
Fe(1)–C(5)	2.052 (5)	C(19)–C(23)	1.538 (7)
Fe(1)–C(6)	2.066 (4)	C(19)–C(24)	1.525 (7)
Fe(1)–C(7)	2.058 (5)	C(20)–C(25)	1.506 (8)
Fe(1)–C(8)	2.051 (5)	C(20)–C(26)	1.544 (7)
Fe(1)–C(9)	2.046 (5)	C(21)–C(27)	1.535 (7)
Fe(1)–C(10)	2.048 (5)	C(21)–C(28)	1.521 (7)
P(1)–C(1)	1.826 (5)	C(22)–C(29)	1.531 (7)
P(1)–C(19)	1.856 (5)	C(22)–C(30)	1.535 (7)

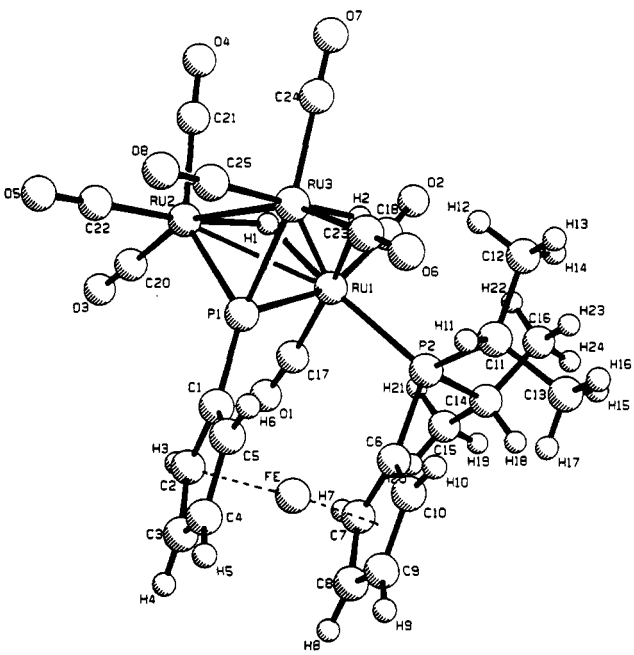

Figure 1. PLUTO plot for **7**.

both Ru(2) and Ru(3) are 7-coordinated and Ru(1) is 8-coordinated. The complex is electron precise. The three Ru–Ru distances within the cluster show a large variation. The two longer ones (Ru(1)–Ru(2) = 2.950 (1) Å and Ru(1)–Ru(3) = 2.984 (2) Å) are bridged by the hydrides. The shortest Ru(2)–Ru(3) distance (2.817 (1) Å) is shorter than that in the parent carbonyl [$Ru_3(CO)_{12}$] (average 2.854 Å). The Ru–C distances of the carbonyl groups that are roughly trans to the phosphinidene group are significantly longer than the others (Ru(2)–C(20) = 1.958 (3) Å, Ru(3)–C(23) = 1.945 (4) Å, Ru(1)–C(18) = 1.941 (3) Å; other Ru–C distances average 1.894 Å) due to the large trans influence of the phosphinidene group. The ferrocenyl bridge is not unusual, and the cyclopentadienyl rings show

Table VII. Intramolecular Bond Angles (deg) for 9 (Esd's in Parentheses)

Ru(3)–Ru(1)–Cl(1)	87.21 (3)	C(16)–Ru(3)–C(18)	94.0 (3)
Ru(3)–Ru(1)–P(1)	170.87 (3)	C(17)–Ru(3)–C(18)	166.1 (2)
Ru(3)–Ru(1)–O(9)	82.5 (1)	Cp(1)–Fe(1)–Cp(2)	171.5 (1)
Ru(3)–Ru(1)–C(11)	82.9 (2)	Ru(1)–Cl(1)–Ru(2)	77.81 (4)
Ru(3)–Ru(1)–C(12)	92.6 (2)	Ru(1)–P(1)–C(1)	119.9 (2)
Cl(1)–Ru(1)–P(1)	92.95 (4)	Ru(1)–P(1)–C(19)	113.8 (2)
Cl(1)–Ru(1)–O(9)	79.8 (1)	Ru(1)–P(1)–C(20)	114.4 (2)
Cl(1)–Ru(1)–C(11)	170.1 (2)	C(1)–P(1)–C(19)	102.2 (2)
Cl(1)–Ru(1)–C(12)	92.7 (2)	C(1)–P(1)–C(20)	100.1 (2)
P(1)–Ru(1)–O(9)	88.5 (1)	C(19)–P(1)–C(20)	104.5 (2)
P(1)–Ru(1)–C(11)	96.9 (2)	Ru(2)–P(2)–C(6)	118.2 (1)
P(1)–Ru(1)–C(12)	96.5 (2)	Ru(2)–P(2)–C(21)	117.3 (2)
O(9)–Ru(1)–C(11)	99.3 (2)	Ru(2)–P(2)–C(22)	112.1 (2)
O(9)–Ru(1)–C(12)	171.2 (2)	C(6)–P(2)–C(21)	103.9 (2)
C(11)–Ru(1)–C(12)	87.2 (3)	C(6)–P(2)–C(22)	99.6 (2)
Ru(3)–Ru(2)–Cl(1)	86.94 (3)	C(21)–P(2)–C(22)	103.4 (2)
Ru(3)–Ru(2)–P(2)	173.12 (3)	Ru(1)–O(9)–Ru(2)	95.8 (1)
Ru(3)–Ru(2)–O(9)	82.5 (1)	P(1)–C(1)–C(2)	124.7 (4)
Ru(3)–Ru(2)–C(13)	83.2 (2)	P(1)–C(1)–C(5)	126.8 (4)
Ru(3)–Ru(2)–C(14)	90.1 (2)	P(2)–C(6)–C(7)	125.1 (4)
Cl(1)–Ru(2)–P(2)	94.24 (4)	P(2)–C(6)–C(10)	126.6 (4)
Cl(1)–Ru(2)–O(9)	79.2 (1)	Ru(1)–C(11)–O(1)	177.0 (5)
Cl(1)–Ru(2)–C(13)	170.1 (2)	Ru(1)–C(12)–O(2)	179.5 (6)
Cl(1)–Ru(2)–C(14)	94.1 (2)	Ru(2)–C(13)–O(3)	176.7 (5)
P(2)–Ru(2)–O(9)	91.0 (1)	Ru(2)–C(14)–O(4)	177.7 (5)
P(2)–Ru(2)–C(13)	95.5 (2)	Ru(3)–C(15)–O(5)	177.9 (6)
P(2)–Ru(2)–C(14)	96.5 (2)	Ru(3)–C(16)–O(6)	178.4 (8)
O(9)–Ru(2)–C(13)	99.0 (2)	Ru(3)–C(17)–O(7)	176.3 (6)
O(9)–Ru(2)–C(14)	170.3 (2)	Ru(3)–C(18)–O(8)	179.3 (5)
C(13)–Ru(2)–C(14)	86.4 (2)	Ru(1)–O(9)–H(1)	120 (4)
Ru(1)–Ru(3)–Ru(2)	67.00 (2)	Ru(2)–O(9)–H(1)	115 (4)
Ru(1)–Ru(3)–C(15)	164.9 (2)	P(1)–C(19)–C(23)	112.4 (4)
Ru(1)–Ru(3)–C(16)	95.8 (2)	P(1)–C(19)–C(24)	110.7 (3)
Ru(1)–Ru(3)–C(17)	95.3 (2)	C(23)–C(19)–C(24)	111.8 (5)
Ru(1)–Ru(3)–C(18)	83.3 (2)	P(1)–C(20)–C(25)	112.8 (4)
Ru(2)–Ru(3)–C(15)	97.9 (2)	P(1)–C(20)–C(26)	113.7 (4)
Ru(2)–Ru(3)–C(16)	162.8 (2)	C(25)–C(20)–C(26)	109.9 (5)
Ru(2)–Ru(3)–C(17)	84.4 (2)	P(2)–C(21)–C(27)	112.0 (4)
Ru(2)–Ru(3)–C(18)	83.9 (2)	P(2)–C(21)–C(28)	112.0 (3)
C(15)–Ru(3)–C(16)	99.3 (3)	C(27)–C(21)–C(28)	111.0 (4)
C(15)–Ru(3)–C(17)	93.0 (2)	P(2)–C(22)–C(29)	110.3 (3)
C(15)–Ru(3)–C(18)	95.8 (2)	P(2)–C(22)–C(30)	114.5 (4)
C(16)–Ru(3)–C(17)	95.1 (3)	C(29)–C(22)–C(30)	109.8 (5)

little variation in C–C distances and C–C–C angles. The two rings are almost eclipsed and have a dihedral angle of 4.21°. The Ru–P bond is longer for the phosphine (P(2)–Ru(1) = 2.359 (1) Å) than for the phosphinidene (average P(1)–Ru = 2.295 (1) Å). Overall, the structure of **7** is similar to that of the previously known $Ru_3(CO)_8(H)_2(\mu_3\text{-PPh})(PPh_3)$,[11] except that in this example the phosphine is situated below the Ru_3 plane in an axial position rather than in the equatorial position of P(2) in **7**.

The $^{31}P\{^1H\}$ NMR spectrum of **7** (Table VIII) shows two signals at 67.5 and 269.4 ppm. This is fully consistent with the structure. The phosphine resonance is shifted 26 ppm from that of the parent complex (δ 41.3 ppm). The phosphinidene phosphorus shows a downfield shift of 228 ppm from that of the parent complex, and the chemical shift is typical of analogous phosphinidene complexes.

Characterization of Compound 6. We were unable to obtain X-ray-quality crystals of this compound; therefore, the characterization is based on spectroscopic data and reactivity studies. The FAB mass spectrum shows the parent ion at m/e 905, corresponding to the loss of two CO groups and one propene molecule from the starting material, **5**. Other ions associated with the loss of eight CO groups support this thesis. The $^{31}P\{^1H\}$ NMR spectrum

(11) Mays, M. J.; Taylor, P. L.; Henrick, K. *Acta Crystallogr.* **1982**, *B38*, 2261.

Scheme I

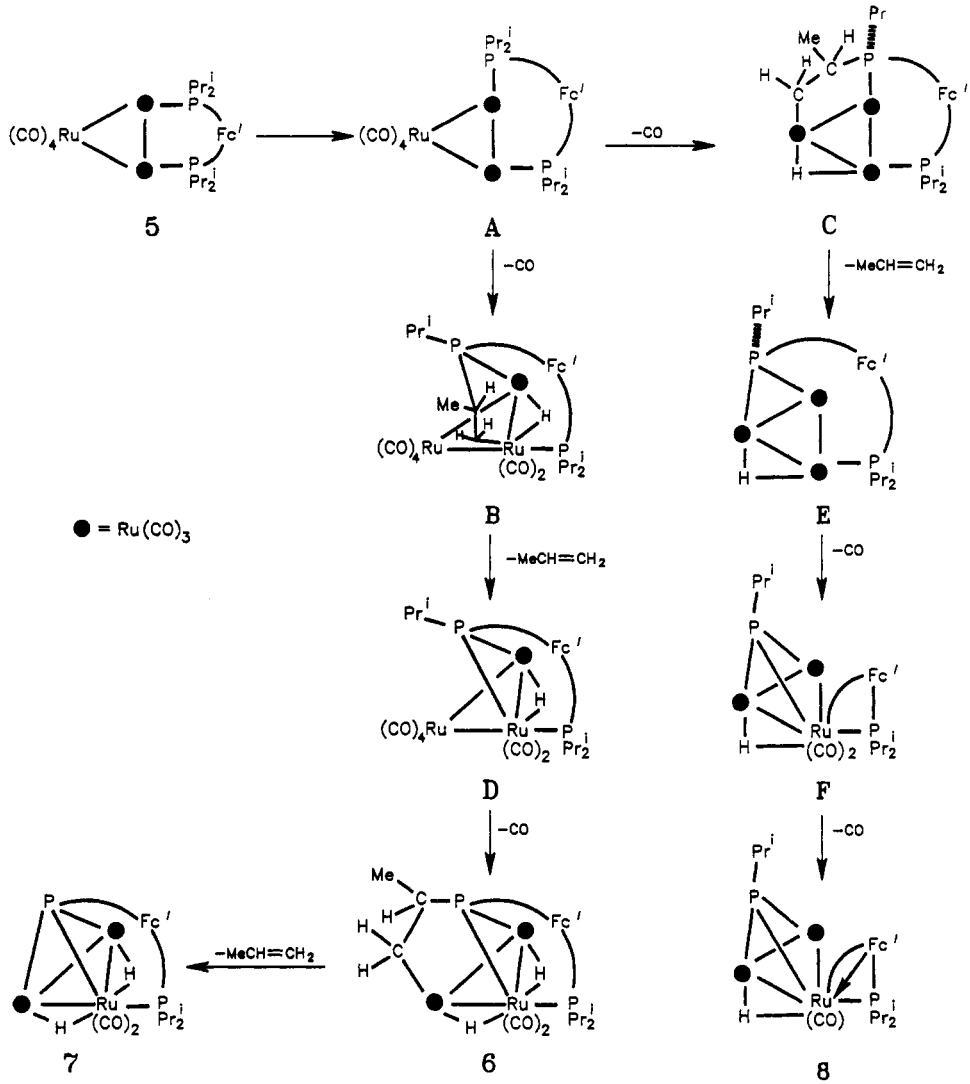

Table VIII. Spectroscopic Results for 6–9

	^{1}H NMR, δ	^{31}P NMR, δ	FAB mass spectrum, m/e
6	4.8 (m, 1 H), 4.58 (m, 2 H), 4.32 (m, 1 H), 4.0 (m, 2 H), 3.94 (m, 1 H), 3.85 (m, 1 H), 2.85 (m, 1 H), 2.58 (m, 2 H), 1.2–1.8 (m, very complex, 17 H), -14.95 (ddd, J_1 = 32.4, J_2 = 19.2, J_3 = 1.8 Hz, 1 H), -15.45 (dd, J_1 = 16.4, J_2 = 9.5, J_3 = 1.8 Hz, 1 H)	73.7, 177.4	905, 849 (base peak), 821, 793, 765, 749, 737, 721, 709, 693, 663, 650, 619, 590, 550
7	1.2–1.5 (m, 12 H), 2.05–2.20 (m, 1 H), 2.20–2.35 (m, 1 H), 4.22–4.45 (m, 1 H, 2 H), 4.52–4.60 (m, 1 H), 4.88–5.00 (m, 2 H, 1 H), 5.14–5.22 (m, 1 H), -18.50 (ddd, J_1 = 33.3, J_2 = 15.6, J_3 = 2.0 Hz), -19.23 (ddd, J_1 = 21.3, J_2 = 9.0, J_3 = 2.0 Hz)	67.5, 269.4	863, 835, 807, 779, 749 (base peak), 721, 706, 693, 678, 665, 650, 622, 604, 591, 565, 550
8	1.85–2.10 (m, 12 H), 1.6–1.7 (m, 6 H), 2.4–2.6 (m, 2 H), 2.95 (m, 1 H), 3.22 (m, 1 H), 3.37 (m, 1 H), 3.50 (m, 1 H), 3.75–3.90 (m, 1 H), 4.9 (m, 2 H), 5.2 (m, 1 H), 5.25 (m, 1 H), -21.0 (dd, J_1 = 22.8, J_2 = 9.0 Hz, 1 H)	53.7, 429.3	849, 821, 793, 765, 737
9	1.0–1.4 (m, 24 H), 2.1–2.4 (m, 4 H), 4.4–4.5 (m, 6 H), 4.95–5.0 (m, 2 H)	20.9	999, 943, 915, 887, 859 (base peak), 815

shows the presence of a phosphine (73.7 ppm) and phosphido group (177.4 ppm). The ^{1}H NMR spectrum shows eight protons in the ferrocenyl region, indicating that the two hydrides (-14.95, -15.45 ppm) do not originate from the C_5 rings. Thus, two possible formulas can be proposed that agree with the analytical and spectroscopic data: $Ru_3(CO)_8(H)_2[Fe(\eta\text{-}C_5H_4PPr^i_2)(\eta\text{-}C_5H_4P\text{-}CHMeCH_2)]$ (**6a**) and $Ru_3(CO)_8(H)_2[Fe(\eta\text{-}C_5H_4PPr^i_2)(\eta\text{-}C_5H_4P\text{-}CMe_2)]$ (**6b**).

The pyrolysis of **6** under the same conditions used for the decomposition of **5** (cyclohexane, 10 h) affords **7** exclusively, and **7** is stable to further change. TLC monitoring reveals no intermediates in this transformation, and simple elimination of propene from **6a** would account for this observation. This more plausible structure for **6**, which accounts for all the data, is shown in Scheme I.

Characterization of Compound 8. Complex **8** is less stable than **6** or **7** in solution, but it can be chromatographed in air without degassing the solvents. The spectroscopic data show the presence of one hydride at -21.0 ppm and two phosphorus atoms, one phosphine, and one phosphinidine. The spectrum in the ferrocene region shows the presence of eight protons, but the pattern is

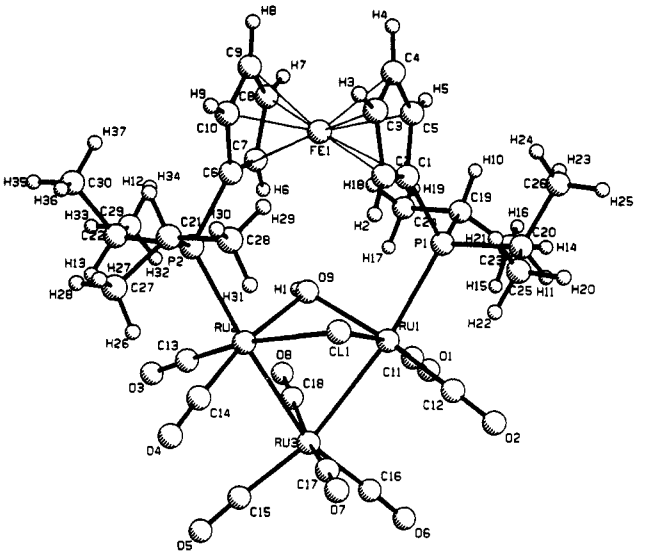

Figure 2. PLUTO plot for **9**.

unusual. Fortunately, we have recently characterized the analogous osmium complex **10**.[12] This novel derivative

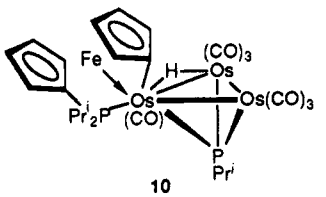

10

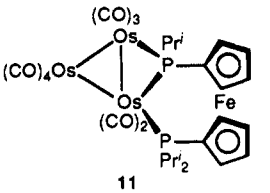

11

contains a metalated C_5 ring that is bound to an osmium atom. There is also an Fe→Os bond involving the same osmium atom. The ^1H NMR spectra of **10** and **8** are very similar. For example, in the ferrocene region we find δ 5.26 (1 H), 5.20 (1 H), 4.88 (2 H), 3.51 (1 H), 3.37 (1 H), 3.22 (1 H), and 2.96 (1 H) for **8** and 5.21 (1 H), 5.16 (1 H), 4.88 (1 H), 4.85 (1 H), 3.72 (1 H), 3.53 (1 H), 3.24 (1 H), and 2.88 (1 H) for **10**. The multiplets associated with the $HCMe_2$ group are at δ 3.81 (1 H) and 2.50 (2 H) for **8** and 3.66 (1 H), 2.58 (1 H), and 2.08 (1 H) for **10**. The data provide strong evidence that **8** and **10** have the same basic structure.

Thermolysis Pathways. Scheme I outlines pathways that account for the formation of **6**–**8**. Similar schemes have been proposed for the thermolysis of $Ru_3(CO)_{10}Fc'(PPh_2)_2$.[4a] The first step is the movement of one end of the ligand from an equatorial to an axial position to afford A. This permits γ-CH activation (β-CH with respect to phosphorus) to take place to afford B or C. The elimination of propene results in the formation of D and E, respectively.

Although D and E were not isolated, there is strong support for the structure of D; the corresponding osmium compound **11** has been isolated and fully characterized.[12] In D the unique isopropyl group on the phosphido group is directed toward the third ruthenium atom. In E it is not. Further γ-CH activation of D affords **6**, whose

Scheme II

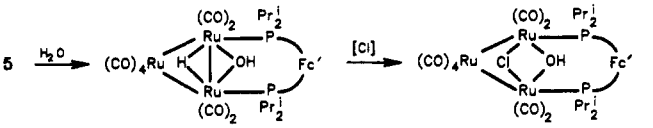

G **9**

characterization is described above. Elimination of propene from **6** affords **7**.

Returning to E, activation of the unique isopropyl group is not possible, and further breakdown apparently takes place via P–C_5-ring cleavage. This is associated with an oxidative addition to afford F; establishment of the Fe→Ru bond ultimately gives **8**. Thus, overall, Scheme I provides a satisfactory rationale for the formation of **6**–**8**.

Characterization of Compound 9. Finally we turn to compound **9**, isolated in low yield from the original pyrolysis experiment; its crystal structure is shown in Figure 2. The basic skeleton is an open Ru_3 triangle with $Fc'(PPr^i_2)_2$, Cl, and OH groups bridging the open side. The two Ru–Ru bond lengths, 2.8444 (6) and 2.8506 (7) Å, are similar to those of $Ru_3(CO)_{12}$ (2.854 Å). Each Ru metal center is 6-coordinated and is octahedral. The spectroscopic properties listed in Table VIII are consistent with this structure.

Complex **9** can be isolated by following the same workup procedure, even when **5** is refluxed in hexane (15 h), conditions that do not result in the formation of **6**–**8**. When a trace amount of water is added to the hexane and the reaction is repeated, the product mixture contains one new compound in low yield and the $^{31}P\{^1H\}$ NMR spectrum of the mixture in toluene-d_8 shows a new resonance at 48.0 ppm. The ^1H NMR spectrum shows a hydride resonance at −17.38 ppm (dd, J = 15.73, J_2 = 11.63 Hz). When the same sample is examined in $CDCl_3$ solution, the resonances of the (Cl)(OH)-bridged complex **9** are recorded. These results suggest that the reaction sequence shown in Scheme II takes place. The source of Cl is probably HCl in the chlorinated solvents used for chromatography or the solvents themselves. The low yield of the reaction has mitigated against further investigation.

There appear to be no descriptions of di(tertiary phosphine)-bridged analogues of G or **9** in the literature. Clusters of the type $Ru_3(CO)_{10}HX$ (X = SR, NHR) are known,[13] as is $Os_3(CO)_{10}(H)(OH)$.[14]

Acknowledgment. We are grateful to the Natural Sciences and Engineering Research Council of Canada for financial support (W.R.C.) and to the University of British Columbia for a graduate fellowship (T.Z.). We thank Johnson-Matthey for the loan of ruthenium salts.

Supplementary Material Available: Tables of anisotropic thermal parameters, torsion angles, and least-squares planes and stereo ORTEP diagrams for **7** and **9** and a table of hydrogen atom positional parameters for **9** (25 pages); tables of measured and calculated structure-factor amplitudes for **7** and **9** (114 pages). Ordering information is given on any current masthead page.

(12) Cullen, W. R.; Rettig, S. J.; Zheng, T. *Organometallics*, in press.

(13) Bruce, M. I. In *Comprehensive Organometallic Chemistry*; Wilkinson, G., Stone, F. G. A., Abel, E. W., Eds.; Pergamon: Oxford, England, 1982; Vol. 4, pp 843–887.

(14) E.g.: Dossi, C.; Fusi, A.; Pizzotti, M.; Psavo, R. *Organometallics* **1990**, *9*, 1994.